The EMBO Journal Vol.18 No.4 pp.977–991, 1999

Assembly requirements of PU.1–Pip (IRF-4) activator complexes: inhibiting function *in vivo* using fused dimers

Abraham L.Brass[1,2], Anne Q.Zhu[1] and Harinder Singh[1,2,3]

[1]Howard Hughes Medical Institute and [2]Department of Molecular Genetics and Cell Biology, The University of Chicago, 5841 S. Maryland Avenue, MC1028, Chicago IL 60637, USA

[3]Corresponding author
e-mail: hsingh@midway.uchicago.edu

Gene expression in higher eukaryotes appears to be regulated by specific combinations of transcription factors binding to regulatory sequences. The Ets factor PU.1 and the IRF protein Pip (IRF-4) represent a pair of interacting transcription factors implicated in regulating B cell-specific gene expression. Pip is recruited to its binding site on DNA by phosphorylated PU.1. PU.1–Pip interaction is shown to be template directed and involves two distinct protein–protein interaction surfaces: (i) the ets and IRF DNA-binding domains; and (ii) the phosphorylated PEST region of PU.1 and a lysine-requiring putative α-helix in Pip. Thus, a coordinated set of protein–protein and protein–DNA contacts are essential for PU.1–Pip ternary complex assembly. To analyze the function of these factors *in vivo*, we engineered chimeric repressors containing the ets and IRF DNA-binding domains connected by a flexible POU domain linker. When stably expressed, the wild-type fused dimer strongly repressed the expression of a rearranged immunoglobulin λ gene, thereby establishing the functional importance of PU.1–Pip complexes in B cell gene expression. Comparative analysis of the wild-type dimer with a series of mutant dimers distinguished a gene regulated by PU.1 and Pip from one regulated by PU.1 alone. This strategy should prove generally useful in analyzing the function of interacting transcription factors *in vivo*, and for identifying novel genes regulated by such complexes.

Keywords: Ets/immunoglobulin/repressor/ternary complex

Introduction

In eukaryotes, gene expression appears to be regulated by the assembly of distinct combinations of transcription factors at promoters and enhancers. The ability of transcription factors to interact specifically with one another, resulting in the formation of hetero-oligomeric complexes, is an important eukaryotic adaptation that enables the generation of diverse inducible and developmentally regulated programs of gene expression. According to this view, a relatively small set of transcription factors can form an exponentially larger population of distinct multi-protein complexes, thereby facilitating the differential regulation of as many as 100 000 genes in a single organism (reviewed by Carey, 1998). Biochemical and functional characterization of transcription factor complexes has shown that the structural information necessary for their assembly is provided by both protein–protein and protein–DNA contacts. Examples of combinatorial interactions include the cooperative binding of the homeodomain protein, MATα2, with the MADS box protein, MCM-1, to regulatory sites controlling mating type in *Saccharomyces cerevisiae* (Bender and Sprague, 1987; Tan and Richmond, 1998), the recruitment of the Ets protein, SAP-1, to the c-fos promoter by the serum response factor, SRF (Dalton and Treisman, 1992), and the binding of a Fos–Jun heterodimer (AP-1) along with the nuclear factor of activated T cells (NFAT) to composite elements in T cell activation genes (Jain *et al*., 1992; Chen *et al*., 1998). Similar principles of interaction regulate the cooperative assembly of high mobility group (HMG) protein-containing multi-activator complexes on the interferon-β (IFN-β) gene promoter (Thanos and Maniatis, 1995) and the T cell receptor-α gene enhancer (Giese *et al*., 1995). The concept of combinatorial control of transcription in higher eukaryotes is supported primarily by transient reporter assays *in vivo* and analysis of protein–DNA interactions *in vitro*. However, the role of combinatorial interactions in regulating the activity of endogenous genes remains to be tested. In part, this stems from the lack of a general approach for assaying the functions of interacting transcription factors *in vivo*.

The lymphoid-restricted interferon regulatory factor, Pip (IRF-4), and the hematopoietic-specific Ets protein, PU.1, form complexes in B cells on composite elements present in immunoglobulin light chain (IgL) gene enhancers (Pongubala *et al*., 1992; Eisenbeis *et al*., 1993). In transient assays, these elements have been shown to be essential for enhancer activity. When co-expressed ectopically, PU.1 and Pip synergistically activate transcription of a reporter gene containing multiple copies of the composite element from the IgL λ enhancer, $E_{\lambda 2\text{-}4}$ (Eisenbeis *et al*., 1995). However, the role of PU.1–Pip complexes in regulating the expression of endogenous IgL genes remains to be elucidated. PU.1–Pip ternary complexes also assemble on the promoter of the *CD20* gene, which encodes a protein implicated in B cell activation (Himmelmann *et al*., 1997). In each instance, the binding of Pip to DNA is dependent on DNA-bound PU.1, which must be phosphorylated on Ser148 (pSer148; Pongubala *et al*., 1993). A C-terminal regulatory domain within Pip itself is also required for ternary complex assembly (Brass *et al*., 1996). In addition, this regulatory domain autoinhibits binding of Pip to DNA in the absence of PU.1. Fusion of this regulatory domain to the DNA-binding domain (DBD) of a related IRF produced a chimeric protein with PU.1-dependent DNA-binding activity. Therefore, this domain contains structural determinants

important for both PU.1 interaction and autoinhibition (Brass *et al*., 1996). The nature of these determinants remains to be defined.

Within the IRF family, Pip is most closely related to the interferon consensus sequence-binding protein (ICSBP). ICSBP is a lympho-myeloid-restricted repressor of interferon-inducible gene transcription (Driggers *et al*., 1990; Nelson *et al*., 1993). Similarly to Pip, ICSBP also binds to Ets–IRF composite elements (EICE) in a PU.1-dependent manner (Eisenbeis *et al*., 1995). However, unlike Pip, ICSBP does not contain an activation domain and, therefore, PU.1–ICSBP complexes are less potent activators (Sharf *et al*., 1995; Brass *et al*., 1996). ICSBP and Pip can each form complexes on an EICE with the lymphoid-restricted Ets protein, Spi-B, a homolog of PU.1 (Ray *et al*., 1992; Su *et al*., 1996; Brass, 1998). These ternary complexes are dependent on the presence of a phosphoserine in Spi-B (pSer149), and mutations in Pip which prevent interactions with PU.1 also block association with Spi-B, suggesting a common mechanism of complexation (Brass, 1998). Thus, based on the expression patterns of PU.1, Spi-B, Pip and ICSBP, up to four combinations of Ets–IRF ternary complexes can regulate gene expression in B cells, while in myeloid cells only PU.1–ICSBP complexes can assemble on target genes.

Gene targeting has shown that while Pip is dispensable for antigen-independent lymphoid development, it is essential for B and T cell activation (Mittrucker *et al*., 1997). B cells from Pip-deficient mice cannot produce antibodies in response to infection, and T cells from these animals are defective in cytotoxic and antitumor capabilities. In addition, Pip is overexpressed in T cells infected with human T-cell leukemia virus-1 (HTLV-1) and may, therefore, be involved in viral-mediated cellular transformation and the resulting adult T cell leukemia (ATL; Yamagata *et al*., 1996). Further evidence for Pip-mediated oncogenesis comes from studies showing that Pip is overexpressed in human multiple myeloma cell lines, due to a chromosomal translocation (Iida *et al*., 1997). Mice deficient in ICSBP demonstrate increased sensitivity to viral infection and exhibit a chronic myelogenous leukemia-like syndrome, suggesting that ICSBP may function as a tumor suppressor gene (Holtschke *et al*., 1996). PU.1 is essential for the development of lymphoid and myeloid lineages, while Spi-B is important for B cell activation and survival (Scott *et al*., 1994; Su *et al*., 1997).

Based on the above observations, we postulate that Ets–IRF ternary complexes may play key roles in immunological responses. Therefore, understanding ternary complex assembly should provide insight into both the mechanism and the biological function of combinatorial interactions in gene expression. Here we undertake a series of biochemical studies to elucidate this mechanism, and find that interdependent protein–protein and protein–DNA contacts regulate PU.1–Pip ternary complex assembly. Additionally, to analyze the function of these factors *in vivo*, we engineered chimeric repressors containing the ets and IRF DBDs connected by a flexible POU domain linker. When stably expressed, the wild-type fused dimer strongly repressed the expression of a rearranged immunoglobulin λ gene, thereby establishing the functional importance of PU.1–Pip complexes in B cell gene expression. Comparative analysis of the wild-type dimer with a series of mutant dimers distinguished a gene regulated by PU.1 and Pip from one regulated by PU.1 alone. This strategy should prove generally useful in analyzing the function of interacting transcription factors *in vivo* as well as in identifying novel genes regulated by such complexes.

Results

Multiple residues in Pip's interaction helix are important for both ternary complex formation with PU.1 in vitro and transcriptional synergy in vivo

Previously, using deletion analysis and secondary structure predictions, we suggested that a putative α-helical region (amino acids 399–413) in Pip's C-terminus is important for ternary complex formation with PU.1 (Figure 1A and B; Brass *et al*., 1996). As noted, PU.1 and Pip function as mutually dependent transcriptional activators *in vivo*. We therefore examined the functional importance of Pip's interaction region, by testing a series of C-terminal deletion mutants for transcriptional activation with PU.1. Expression plasmids encoding PU.1 and hemagglutinin (HA)-tagged Pip deletion mutants were co-transfected into NIH 3T3 cells, along with a chloramphenicol acetyltransferase (CAT) reporter construct containing a tetramer of the $E_{\lambda 2\text{-}4}$ composite element (B4-TKCAT; Figure 1A; Eisenbeis *et al*., 1993). Consistent with previous data, PU.1 and Pip (FLPip) synergistically activated transcription (17-fold). Pip deletion mutants which retained the ability to form a ternary complex with PU.1 (1–439 and 1–419; Brass *et al*., 1996; data not shown) stimulated transcription comparable with full-length Pip. Further deletion into the region encompassing the putative α-helix (1–410) severely reduced ternary complex formation and abolished synergistic activation of transcription. Western blotting showed that the Pip deletion mutants were expressed in transfected-cells at equivalent levels (data not shown). Thus, the α-helical region in Pip's C-terminus is important for both interaction with PU.1 *in vitro* and transcriptional synergy *in vivo*.

To analyze the structural determinants required for these activities, we examined the region in Pip (amino acids 389–420) that encompasses this interaction helix, using a series of alanine substitution (AS) mutant proteins (Figure 1B, bottom). Mutagenesis was done in four residue increments, and the *in vitro* translated (IVT) mutant proteins (Figure 1C) were assessed for their ability to form ternary complexes with PU.1 and a probe containing the $E_{\lambda 2\text{-}4}$ composite element (λB; Figure 1D). Equimolar amounts of the IVT Pip proteins were used based on PhosphorImager analysis of SDS–PAGE gels (Figure 1C). The λB composite element (AAAGGAAGTGAAACCA) contains a PU.1-binding site at its 5′ end separated by 2 bp from the Pip-binding site. The alanine substitution of amino acids 397–400 (PipAS397) and 401–404 (PipAS401) within the predicted helix impaired ternary complex formation, resulting in ~1 or 26% binding, respectively, as compared with wild-type Pip (Figure 1D, compare lane 3 with lanes 6 and 7). Furthermore, the region immediately preceding the helix, amino acids 389–392 (PipAS389), was also important for complex formation (17% of wild-type Pip binding; Figure 1D, lanes 3 and 4).

To test the functional properties of these Pip mutants

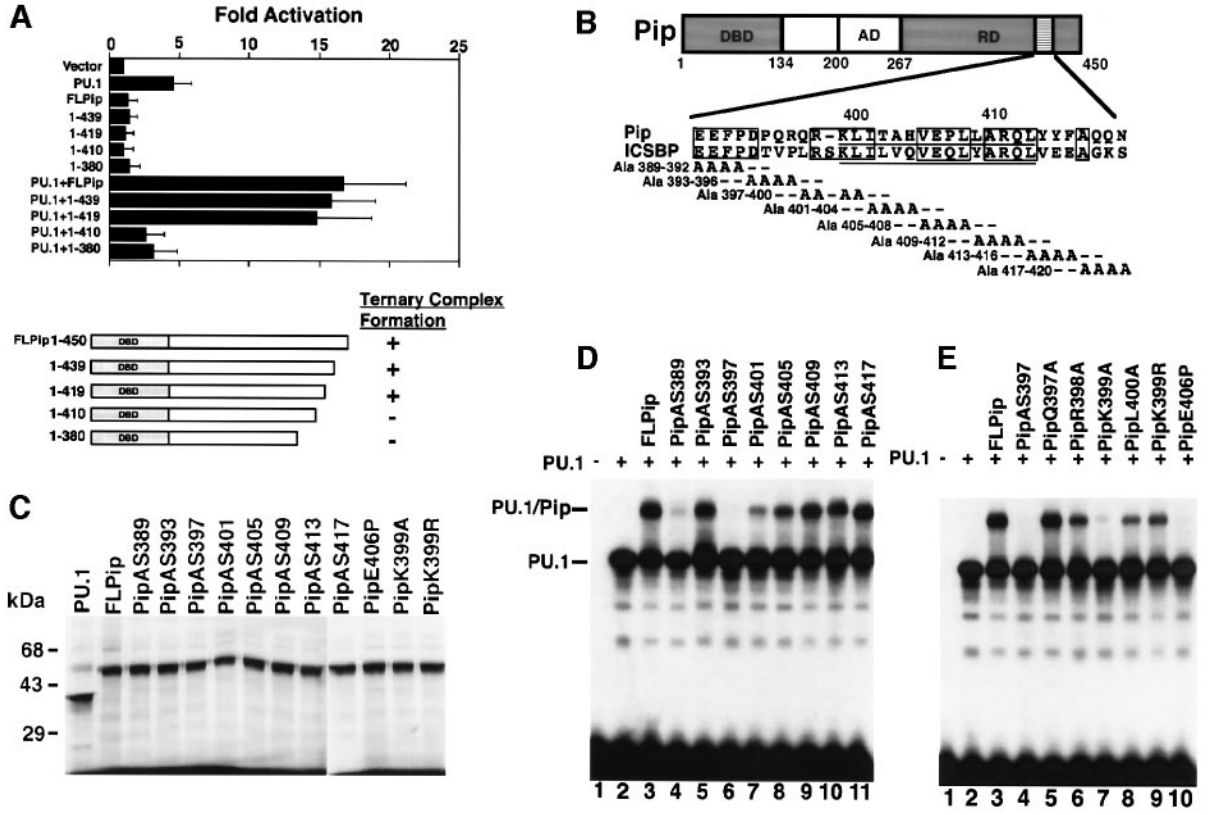

Fig. 1. Multiple residues in Pip's interaction helix are important for ternary complex formation with PU.1 *in vitro* and transcriptional synergy *in vivo*. (**A**) Transient transfection analysis of the indicated Pip C-terminal deletion mutants in NIH-3T3 cells in the absence or presence of PU.1. The reporter construct, B4-TKCAT, contains four copies of the PU.1–Pip composite binding element. Fold-activation (solid bars) indicates CAT activity normalized to the control expression vector and is the average of two independent experiments. Error bars denote standard deviation. The Pip derivatives are schematized below and their respective abilities to form a ternary complex with PU.1 and λB DNA in gel shift assays are indicated in the column as (+) equivalent to wild-type Pip or (–) diminished by at least 10-fold. (**B**) A schematic diagram of the functional domains of Pip. The locations of the DNA-binding domain (DBD), activation domain (AD) and regulatory domain (RD) are shown, based on previous deletion analyses (Brass *et al*., 1996; Brass, 1998). The amino acid sequence encompassing the putative interaction helix in Pip and the homologous region in ICSBP as well as the alanine substitution strategy are shown below. Areas of amino acid sequence identity are boxed and the predicted helix (amino acids 399–413) is underlined. (**C**) SDS–PAGE analysis of [^{35}S]methionine-labeled *in vitro* translated (IVT) Pip mutant proteins used for binding reactions. (**D** and **E**) Gel mobility shift analysis of the indicated IVT Pip alanine substitution (AS) mutant derivatives in the presence of PU.1 with the λB site as a DNA template. Each PipAS mutant contains a clustered substitution of four alanine residues beginning at the indicated position. FLPip refers to the full-length wild-type protein. Equimolar amounts of the Pip proteins were used based on PhosphorImager analysis of SDS–PAGE gels. The positions of the PU.1 and PU.1–Pip protein–DNA complexes are indicated on the left.

(AS393–AS413), we assayed for transcriptional activation in conjunction with PU.1, as described above. Consistent with the biochemical analysis, PipAS397 was least effective in stimulating transcription (Table I). Partial activation of transcription by this mutant protein may be due to its ability to associate weakly with PU.1 and DNA through an interaction between the IRF and ets DBDs (see below). The increasing ability of the PipAS401, 405 and 409 proteins to stimulate transcription correlated with increasing propensity for ternary complex formation (Figure 1D; Table I). Western blot analysis of transfected cell lysates showed that the wild-type and Pip mutant proteins were expressed at comparable levels (data not shown). Therefore, the structural determinants of Pip that are important for ternary complex assembly are also required for transcriptional activation *in vivo*.

To examine residues in the predicted α-helix important for PU.1 interaction, we assayed single alanine substitutions of amino acids 397–400, since this region was essential for complex formation. This experiment showed that Lys399 was important for ternary complex formation, as its substitution by alanine resulted in 8% of wild-type complex assembly (Figure 1E, lane 7). A substantial retention of wild-type binding (40%) was seen after substitution of an arginine for lysine at that position (Figure 1E, compare lanes 9 and 3). Alanine subsitutions of Arg398 and Leu400 also diminished complexation (45 or 31% of wild-type binding levels; Figure 1E, compare lane 3 with lanes 6 and 8). Together, these data suggest that multiple side chains within this region may contact PU.1. Next, we attempted to disrupt the folding of the interaction helix by substituting a proline for glutamine at position 406 (PipE406P). This protein has two consecutive proline residues, which should break the presumed α-helix. PipE406P showed severely reduced interaction with PU.1 (2% of wild-type levels; Figure 1E, compare lane 10 with lane 3). Importantly, mutation of this Glu406 to an alanine had no effect on ternary complex formation, indicating that the nature of the side chain was not critical (data not shown). Taken together, these observations suggest that the predicted α-helix is essential for PU.1–Pip interaction.

As noted, previous deletion analysis suggested that Pip's interaction helix was also required for autoinhibition of DNA binding (Brass *et al*., 1996). To determine residues

Table I. PU.1-dependent transcriptional activation by Pip AS mutant proteins

Expression vector	Fold activation ± SD
Vector	1
PU.1	4.5 ± 0.7
PU.1 + FLPip	24.5 ± 2.1
PU.1 + PipAS393	20.5 ± 0.6
PU.1 + PipAS397	9.0 ± 1.4
PU.1 + PipAS401	13.5 ± 0.7
PU.1 + PipAS405	19.5 ± 2.0
PU.1 + PipAS409	23.0 ± 1.4
PU.1 + PipAS413	19.0 ± 1.6

NIH 3T3 cells were co-transfected with the B4-TKCAT reporter and the indicated expression vectors. Cell lysates were analyzed for CAT activity 48 h post-transfection. Fold activation indicates CAT activity normalized to the control expression vector and is the average of two independent experiments. SD, standard deviation.

important for autoinhibition, we compared the DNA binding of alanine substitution mutants with wild-type Pip using gel shift assays with reduced levels of the non-specific DNA-binding competitor, poly(dI–dC) (Figure 2A). Independent DNA binding by Pip deletion mutants is inhibited by high concentrations of poly(dI–dC) (Brass *et al*., 1996). As shown previously, full-length Pip cannot bind to DNA in the absence of PU.1; however, a C-terminal deletion mutant, Pip 1–410, can bind DNA independently (Figure 2A, compare lanes 2 and 3; Brass *et al*.,1996). Alanine substitution mutagenesis of residues 389–420 showed that amino acids 401–408 were specifically required for autoinhibition (Figure 2A, compare lane 2 with lanes 7 and 8). Alanine substitution of amino acids 401–404 and 405–408 resulted in 9- and 15-fold increases in binding above background, respectively. The alanine substitution mutant PipAS389 generated an anomolous rapidly migrating protein–DNA complex. This complex is probably due to a truncated Pip protein produced by partial proteolysis. It should be noted that the majority of this mutant protein is full length (Figure 1C). Mutation of E406 to proline also generated a protein which bound DNA independently (32-fold above background), suggesting that overall helix integrity is necessary for both autoinhibition and ternary complex formation (Figure 2A, compare lanes 2 and 12). Independent DNA binding of these Pip mutants was specific, because they did not recognize a probe containing a mutation in the Pip-binding site, B2 (GAAACC to cgtACC; data not shown). A slower mobility complex (Pip*) was observed in reactions containing mutants which had lost autoinhibition (Figure 2A, lanes 3, 7, 8 and 12). This complex did not form on the B2 probe and was supershifted by anti-Pip antiserum (data not shown), suggesting that it may represent a Pip dimer–DNA complex.

Interestingly, these experiments showed that the structural determinants in Pip required for autoinhibition of DNA binding overlap with, but can be uncoupled from, those required for ternary complex formation. Figure 2B depicts a schematized helix which summarizes these data. In this diagram, we have extended the N-terminus of the interaction helix to include residues 395–398 based on Chou–Fasman secondary structure predictions (Chou and Fasman, 1978; Brass *et al*., 1996). In addition, a predicted loop (amino acids 391–394) immediately preceding the helix is shown. Residues in the center of the helix are required for both

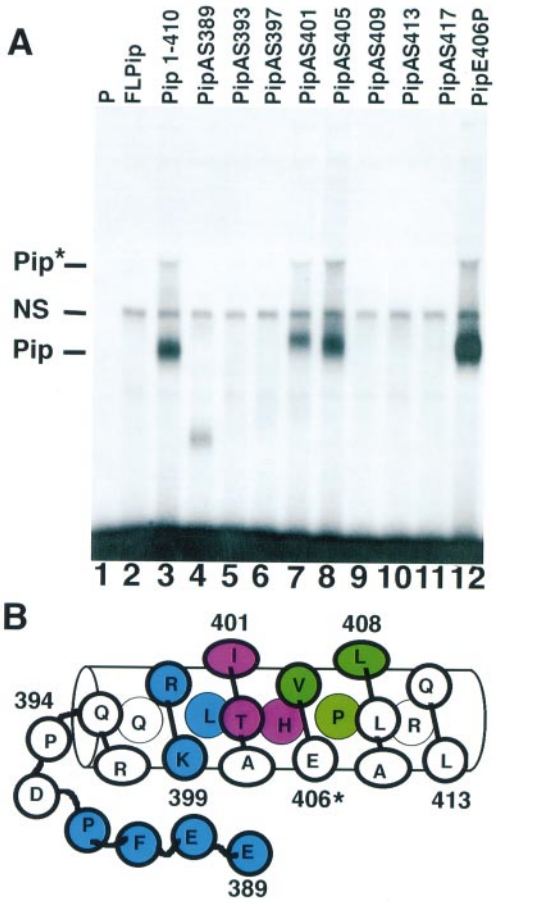

Fig. 2. Structural determinants required for autoinhibition of Pip DNA binding overlap with, but can be uncoupled from, those required for ternary complex formation. (**A**) Gel mobility shift analysis of the indicated IVT Pip alanine substitution mutant derivatives with the λB site as a template. All Pip proteins are present in equimolar amounts. The positions of the Pip–DNA complex (Pip), a possible Pip dimer–DNA complex (Pip*) and a non-specific protein–DNA complex (NS) are shown on the left. P denotes template alone. (**B**) A schematic diagram of a predicted interaction helix and an immediately preceding loop in Pip, summarizing the results of alanine substitution mutagenesis. Blue residues play a role in ternary complex formation. Green residues are important for autoinhibition. Purple residues are important for both ternary complex formation and autoinhibition. E406* indicates that mutation of this residue to a proline impaired both ternary complex formation and autoinhibition. Residues on the back of the predicted α-helix are represented by thinner lines.

autoinhibition and ternary complex formation. The PU.1 interaction surface extends N-terminal of this region to include the helical residues 398–400. In contrast, the autoinhibitory determinants extend in a C-terminal direction to include amino acids 405–408. We note that autoinhibition and ternary complex formation are uncoupled by alanine substitution of residues 397–400. This mutant protein, PipAS397, is defective in its interaction with PU.1, but is autoinhibited.

Pip contains two major structural domains, a DNA-binding domain and a regulatory domain, separated by a linker

Two predictions from our earlier model are (i) the existence of an independently folded C-terminal regulatory domain within Pip and (ii) the ability of Pip to undergo a conformational change upon ternary complex formation (Brass *et al*.,

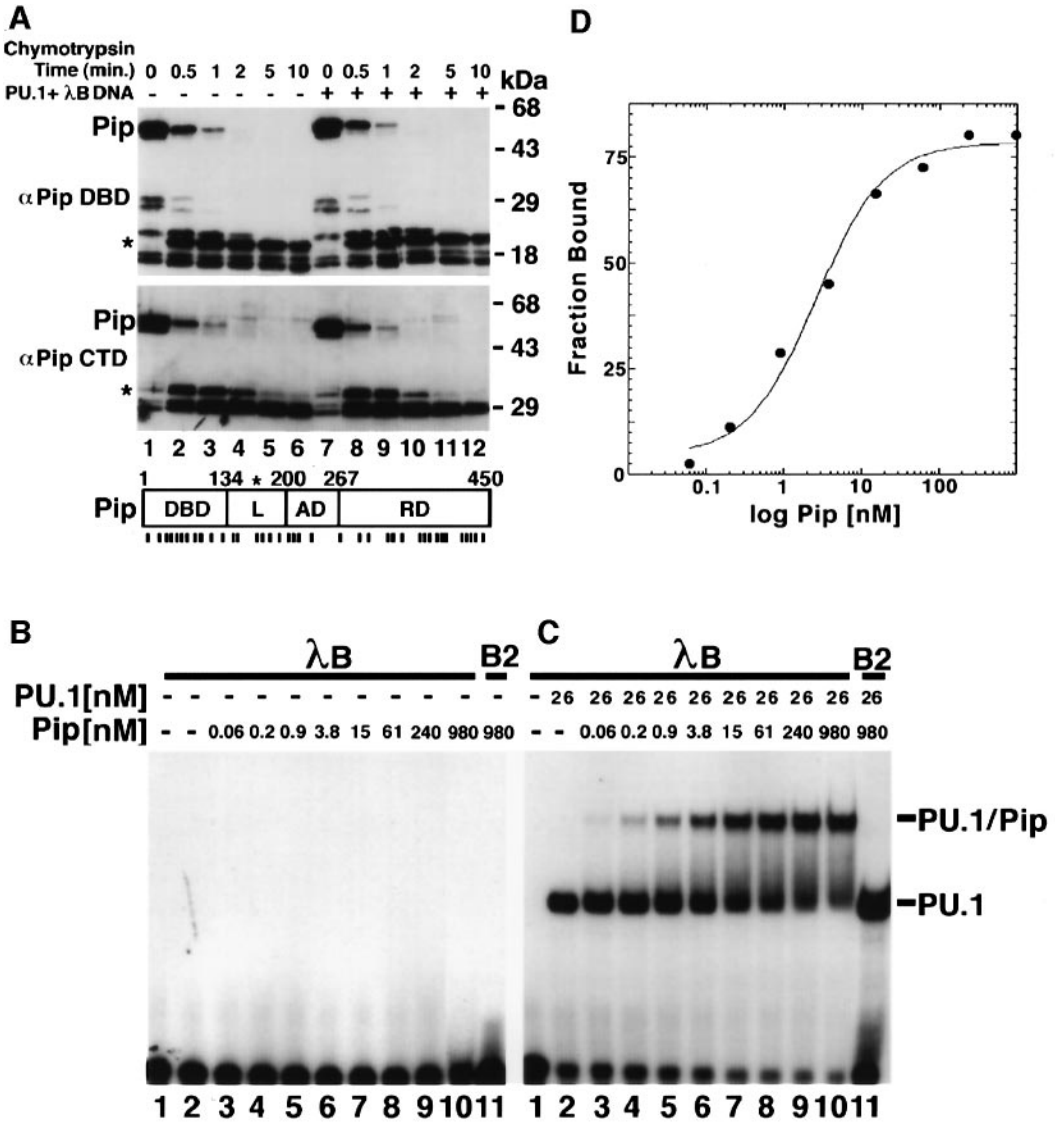

Fig. 3. Pip contains two major structural domains, a DNA-binding domain and a regulatory domain, separated by a linker. (**A**) Affinity-purified recombinant Pip protein (see Materials and methods) was subjected to partial proteolysis with chymotrypsin. Proteolytic fragments were analyzed by Western blotting using anti-Pip DBD (top) or anti-Pip CTD antisera (bottom). The latter antiserum recognizes a C-terminal epitope (amino acids 433–449) in Pip. The time of chymotrypsin digestion is indicated across the top. Chymotryptic digests of Pip were performed in the absence (–) or presence (+) of PU.1 and λB DNA under conditions of efficient ternary complex formation. A schematic diagram of Pip as in Figure 1A; 'L' indicates a protease-sensitive linker region. Vertical lines depict potential chymotrypsin cleavage sites. The asterisk denotes two chymotrypsin cleavage sites mapped in our assays (Tyr169 and Trp178). (**B** and **C**) Quantitative gel mobility shift analysis using affinity-purified Pip protein in the absence (B) or presence (C) of purified recombinant PU.1. λB is the wild-type template, whereas B2 is a variant containing a severe mutation in the Pip-binding site (see Figure 6B). (**D**) Graphical representation of the DNA-binding data shown in (C). Fraction bound denotes the proportion of template contained within the ternary complex.

1996). To test these predictions, we performed partial proteolysis of free Pip or Pip assembled into a ternary complex with PU.1 and λB DNA. To undertake this analysis, full-length Pip was expressed in *Escherichia coli* and affinity purified as a His-tagged fusion protein. His-tagged PU.1 (amino acids 119–272) was expressed and affinity purified from insect cells. This recombinant protein was phosphorylated appropriately and interacted with Pip equivalently to full-length PU.1 generated by *in vitro* translation (see below). Figure 3A shows Western analysis of chymotryptic digests of Pip in the absence (lanes 1–6) or presence (lanes 7–12) of PU.1 and λB DNA. The anti-Pip DBD Western blot detected a major proteolytic-resistant domain of ~20 kDa (top panel, marked by an asterisk). The N-terminus of this fragment was found to be blocked upon sequencing but retained the His tag by Western blotting (data not shown). Therefore, we estimate that this 20 kDa domain comprises the first 180 residues of Pip. Analysis of the same reactions with the anti-Pip C-terminal domain (CTD) antiserum showed the presence of two fairly stable protein fragments which migrated as a doublet of ~32 kDa (bottom panel, marked by an asterisk). N-terminal sequencing of these species revealed that chymotrypsin cleaved after residues Tyr169 or Trp178. Note that the anti-Pip CTD antiserum recognizes an extreme C-terminal epitope (amino acids 433–449).

Therefore, these experiments establish that a functional

regulatory domain, containing the regions necessary for ternary complex formation and autoinhibition, resides within an independently folded protein module (amino acids 170–450). This domain is tethered to the DBD by a protease-sensitive linker (Figure 3A, bottom). As noted above, this experiment also examined potential conformational changes in Pip upon assembly into the ternary complex. No changes in the rate or pattern of proteolysis were detected when Pip was recruited by PU.1 on λB DNA (Figure 3A, compare lanes 1–6 with lanes 7–12). Similar results were obtained using V8 protease, trypsin and thermolysin (data not shown). These data suggest that any PU.1-induced conformational change within Pip occurs by pivoting of Pip's regulatory domain about the flexible linker.

Pip's regulatory domain greatly stimulates DNA binding cooperativity with PU.1

We analyzed the contribution of Pip's regulatory domain to ternary complex assembly by comparing the binding affinity of the full-length protein with that of its DBD. Quantitative gel shift assays were performed with affinity-purified recombinant proteins. Conditions were established to occupy 80% or greater of the λB probe with PU.1, so as to provide maximal PU.1–DNA complexes for interaction with Pip. We observed that the DNA-binding activity of Pip was completely dependent on the presence of PU.1 at all protein concentrations tested (Figure 3B and C). In addition, gel shift assays using the phosphorylation-defective PU.1 mutant, PU.1S148A, showed that the binding of Pip was dependent on the presence of pSer148 (data not shown). The data from gel shift assays allowed us to calculate the equilibrium dissociation constant (K_d) of Pip in the presence of PU.1 to be ~2.6 nM (Figure 3D). This K_d value is likely to be an underestimate, because the binding curve shows that at saturation, ~75% of the recombinant PU.1 interacts with Pip and is therefore phosphorylated appropriately.

Our earlier experiments indicated that PU.1 weakly recruited the Pip DBD to DNA, suggesting the existence of a second structural component of PU.1–Pip cooperativity, not involving Pip's regulatory domain (Brass *et al*., 1996). To explore this observation, we used PU.1 and Pip DBD (amino acids 1–134) proteins in quantitative gel shift assays as described above (Figure 4A and B). Unlike full-length Pip, the isolated Pip DBD possessed intrinsic, albeit weak, DNA affinity (K_d ~ 96 μM, compare Figures 3B and 4A), consistent with removal of the autoinhibitory domain. Binding by Pip DBD was sequence specific since no complex was detected with the mutant B2 probe (data not shown). Pip DBD bound the λB template with higher affinity in the presence of PU.1, K_d ~2.1 μM (Figure 4A and B). Thus, the Pip DBD has a low intrinsic affinity for the λB sequence which is increased 20- to 40-fold by PU.1. We note that the interaction between the isolated DBD of Pip and PU.1 is not dependent on phosphorylation of Ser148 since the phosphorylation-deficient PU.1S148A interacted with the Pip DBD equivalently to PU.1 (data not shown). Furthermore, similar experiments revealed that the isolated ets domain of PU.1 (amino acids 160–272) recruited the Pip DBD to the λB site comparably with the PU.1 protein containing the PEST region (amino acids 119–272, Figure 4C). These data suggest that PU.1 and Pip additionally interact through their DBDs. However, the affinity of full-length Pip for the PU.1–DNA complex is >800-fold greater than that observed for the Pip DBD (2.6 nM versus 2.1 μM). Thus, the interaction of Pip's regulatory domain with the PEST region of PU.1 greatly enhances DNA-binding cooperativity.

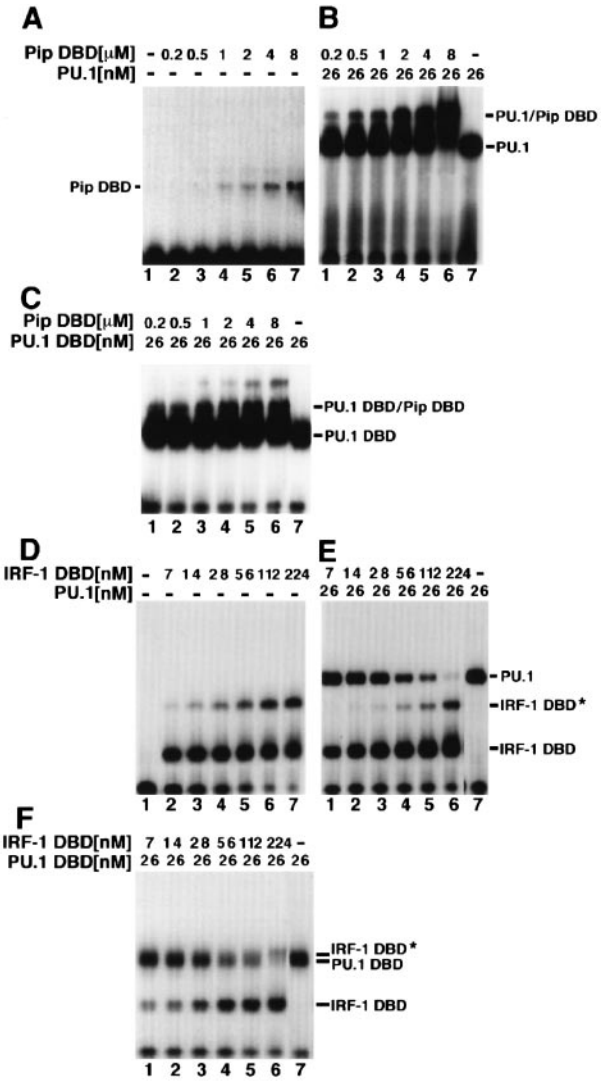

Fig. 4. PU.1 binds cooperatively with the DBD of Pip but competitively with the related DBD of IRF-1. (A–C) Quantitative gel mobility shift analysis using affinity-purified Pip DBD protein in the absence (**A**) or presence of purified recombinant PU.1 (**B**) or PU.1 DBD (**C**) with the λB site as a probe. (D–F) Quantitative gel mobility shift analysis using purified recombinant IRF-1 DBD in the absence (**D**) or presence of purified recombinant PU.1 (**E**) or PU.1 DBD (**F**) with the λB site as a probe. Protein–DNA complexes are indicated along the margins. IRF-1 DBD* indicates a possible IRF-1 DBD dimer–DNA complex.

PU.1 and the DNA-binding domain of IRF-1 compete for binding to λB DNA

To address whether the association between PU.1 and the Pip DBD on λB DNA was specific, we tested the DBD of the prototypic IRF family member, IRF-1 (Harada *et al*., 1988). The IRF domains of Pip and IRF-1 share 43% amino acid identity. Gel shift assays with purified IRF-1 DBD (amino acids 1–113, Escalante *et al*., 1998) were performed in the absence or presence of saturating concentrations of PU.1 or PU.1 DBD (Figure 4D–F). These data

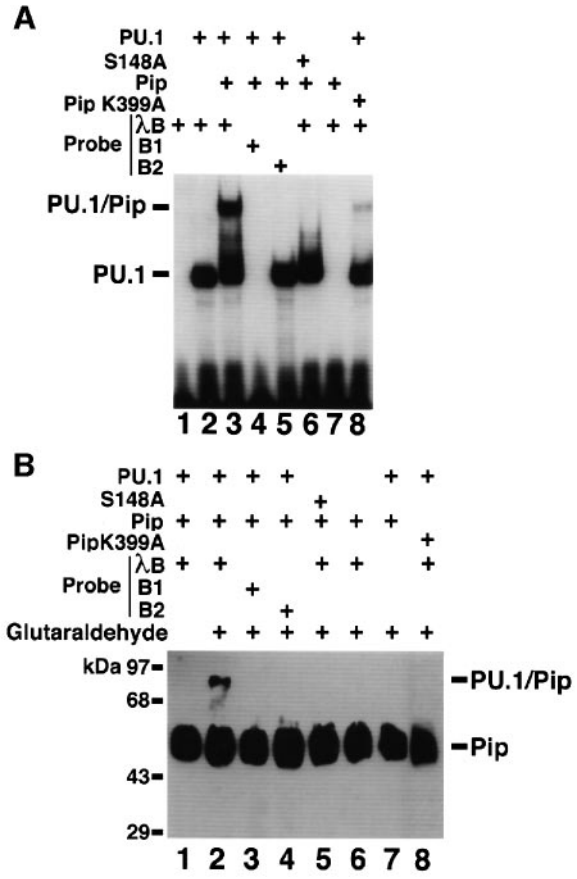

Fig. 5. PU.1 and Pip cross-linking is DNA template dependent. (**A**) Gel mobility shift analysis using the indicated purified proteins and DNA probes. Equimolar amounts of Pip or PipK399A, and PU.1 or PU.1S148A were used in the binding reactions. The B1 and B2 probes contain mutations in the PU.1- and Pip-binding sites, respectively (see Figure 6B). (**B**) DNA-binding reactions using the indicated components were subjected to glutaraldehyde (0.005%) cross-linking. Reaction products were analyzed by Western blotting using anti-Pip antiserum. The positions of Pip and the PU.1–Pip adduct are indicated on the right.

demonstrated: (i) the high DNA affinity of IRF-1's DBD compared with that of the Pip DBD (compare Figure 4D with A, taking note of protein concentrations); (ii) the IRF-1 DBD bound the λB site as both a monomer and a dimer; and (iii) increasing concentrations of the IRF-1 DBD displaced either PU.1 or PU.1 DBD from the λB site. Therefore, the DBDs of IRF-1 and Pip have structurally diverged, such that Pip binds cooperatively with PU.1, while IRF-1 displaces PU.1 from the composite element.

PU.1 and Pip physically associate in a DNA-dependent manner

Our model for ternary complex assembly predicted that direct physical interaction between PU.1 and Pip would be DNA template directed (Brass *et al*., 1996). Therefore, to examine the interaction between PU.1 and Pip, glutaraldehyde cross-linking was performed in the absence or presence of template DNA (Figure 5B). Reaction products were separated by SDS–PAGE and analyzed by Western blotting. A glutaraldehyde-dependent adduct containing Pip was detected, with a molecular mass of ~80–85 kDa, in excellent agreement with the predicted size of a cross-linked species comprising a heterodimer of Pip and PU.1 (Figure 5B, compare lanes 1 and 2). Western blotting using anti-PU.1 antisera showed that this protein adduct also contained PU.1 (data not shown). Formation of the PU.1–Pip protein adduct was dependent on: (i) phosphorylation of Ser148 in PU.1; (ii) Lys399 in Pip's interaction helix; and (iii) λB DNA containing intact PU.1- and Pip-binding sites (Figure 5B, lanes 3–8, probes designated B1 and B2 contain severe mutations in either the PU.1- or Pip-binding sites; detailed in Figure 6B). Therefore, the PU.1–Pip interaction detected by glutaraldehyde cross-linking displayed the same requirements as those determined for ternary complex assembly using the gel shift assay (Figure 5A and B). These results suggest that protein–protein and protein–DNA interactions function coordinately in establishing a specific and stable ternary complex.

Engineering a PU.1–Pip chimeric repressor

As demonstrated above, the protein–protein interactions between Pip and PU.1 are vital for cooperative DNA binding. Based on these observations, we reasoned that by covalently coupling the DBDs of PU.1 and Pip, we might generate a fused dimer whose DNA specificity and affinity are similar to those of the wild-type complex. Since this fused dimer would lack activation domains, we envisaged that *in vivo* it would function as a gene-specific repressor by displacing endogenous PU.1–Pip complexes from composite regulatory elements. Such a repressor could be used to probe the requirement for PU.1–Pip complexes in regulating the transcription of a productively rearranged IgL gene, *in vivo*.

The crystal structure of the PU.1 DBD bound to DNA shows that the N-terminus of PU.1 faces the binding site for Pip (Kodandapani *et al*., 1996). Therefore, we placed the Pip DBD (amino acids 1–150) at the N-terminus of the fusion protein and connected it to the PU.1 DBD (amino acids 160–272) with a linker (26 amino acids) from the POU domain of Oct-2 (Figure 6A). This linker was chosen because it flexibly connects the POU homeo- and POU-specific domains (Herr and Cleary, 1995), and appears unstructured in the Oct-1–DNA co-crystal structure (Klemm *et al*., 1994). Fused dimers lacking or containing tandem copies of the linker were analyzed for their DNA-binding properties (data not shown). Chimeric proteins containing either two or three copies of the linker bound to the λB site with highest affinity. Therefore, the chimera containing two copies of the linker (PipPU) was employed in further analysis.

In gel shift assays using the λB site, PipPU preferred the composite element to one containing only a PU.1 site by a factor of 3 (Figure 6B, compare lane 5, panels λB and B2). However, the binding of PU.1 and Pip to λB was greater than that of the chimera (4-fold), illustrating that on this site the covalent linkage did not fully recapitulate wild-type affinity (Figure 6B, compare lanes 4 and 5, panel λB). The λB probe contains a high affinity PU.1-binding site (AAGGAA), which might mask some of the gain in DNA binding provided by the fusion of the Pip DBD. To test this, gel shifts were done using the composite element from the CD20 promoter, which contains a lower affinity PU.1-binding site (AA**A**GAA; Figure 6B, panel CD20). Consistent with previous data, PU.1 bound with lower affinity to the CD20 site as compared with λB (Figure 6B, lane 2, panels λB and CD20; Himmelman *et al*., 1997).

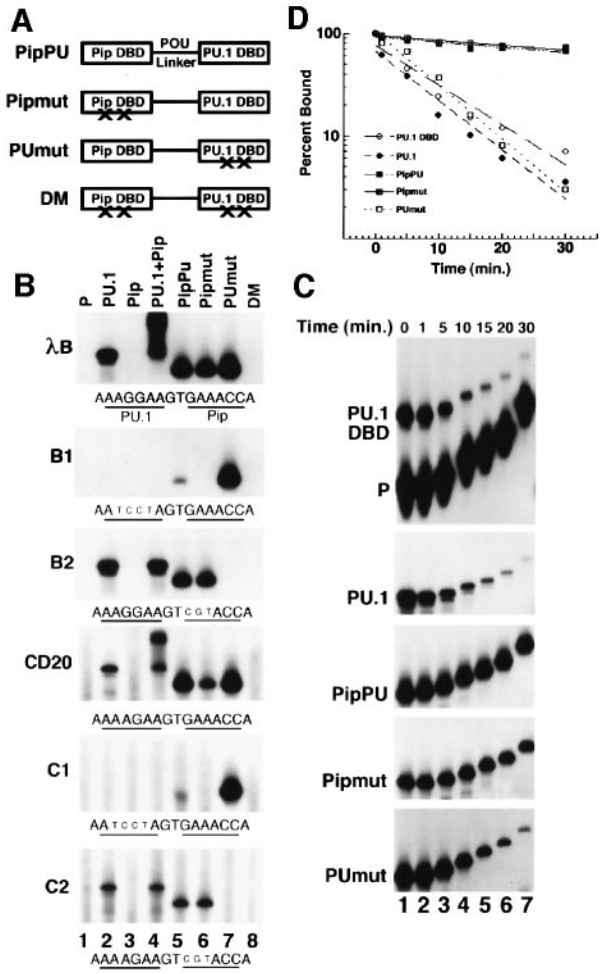

Fig. 6. Fusing the DBDs of Pip and PU.1 generates a chimeric protein which preferentially binds composite elements with increased stability. (**A**) Schematic diagram of the PipPU chimera and its mutant counterparts. The Pip DBD (amino acids 1–150) was fused to the PU.1 DBD (amino acids 160–272) using a tandem repeat of the Oct-2 POU domain linker. Xs indicate alanine substitutions made either in the Pip DBD (R98A and C99A) or PU.1 DBD (R232A and R235A) or both, to create Pipmut, PUmut and DM, respectively. (**B**) Gel mobility shift analysis of the indicated IVT wild-type or mutant chimeric proteins. PU.1 and the chimeric proteins are present in equimolar amounts. The DNA sequence of the composite element of the indicated wild-type or mutant probes is shown below each panel. Mutated bases are shown in smaller type. The PU.1- and Pip-binding sites have been underlined based on methylation interference analysis of the λB site (Eisenbeis *et al*., 1995). Probes B1 and C1 differ in their flanking sequences (Brass *et al*., 1996; Himmelman *et al*., 1997). (**C**) Dissociation of protein–DNA complexes monitored using gel shift assays with the indicated IVT proteins and the λB probe. Binding reactions were permitted to reach equilibrium and then challenged with an excess of unlabeled λB DNA. Aliquots were loaded onto a running gel at the indicated time points. (**D**) Graphical representation of the DNA-binding data shown in (C). The percentage bound represents the proportion of DNA probe that remains bound by the indicated protein at each time point. Probe bound at time zero is set at 100%.

Importantly, the PipPU fused dimer bound the wild-type CD20 site with an 8-fold higher affinity than the C2 mutant site, which contains a mutation in the Pip-binding site (Figure 6B, lane 5, panels CD20 and C2). On the CD20 element, PipPU bound with comparable affinity to PU.1 and Pip (Figure 6B, compare lanes 4 and 5, panel CD20), thus demonstrating that on certain composite elements, fusion of the two DBDs can recapitulate the affinity of the PU.1–Pip complex.

Mutant chimeric proteins were constructed to evaluate the role of the individual DBDs in the fused dimer (Figure 6A). Alanines were substituted for two critical residues within the respective recognition helices of either PU.1 (R232A and R235A; Kodandapani *et al*., 1996) or Pip (R98A and C99A; Escalante *et al*., 1998), or both, and these chimeric proteins were tested for binding to the λB and CD20 sites. As expected, the Pip mutant (Pipmut) exhibited reduced affinity for the composite sites, and therefore its binding properties resembled those of PU.1 (Figure 6B, compare lanes 2 and 6). Surprisingly, the PU.1 mutant (PUmut) bound the λB and CD20 sites with affinity similar to the wild-type fused dimer (Figure 6B, compare lanes 5 and 7, λB and CD20). Although the DNA affinity of PUmut was comparable with that of PipPU, its DNA specificity was quite different. Unlike PipPU, the binding of PUmut to the composite element was strictly dependent on the Pip binding site (Figure 6B, lane 7, panels B1 and B2). Importantly, the double mutant (DM) fused dimer did not interact detectably with the composite sites (Figure 6B, lane 8).

To examine the stabilities of the protein–DNA complexes formed by PU.1 and the fused dimers, dissociation rates were determined. In these experiments, binding reactions were permitted to reach equilibrium, at which point the DNA–protein complexes were challenged with excess unlabeled DNA. Decay of the DNA–protein complexes was monitored by loading aliquots on a running gel at timed intervals (Figure 6C). The half-life of each complex was calculated using an exponential decay plot (Figure 6D). The estimated half-life for the PipPU–DNA complex (60 min) was considerably longer than that for PU.1 (6 min) or the PU.1 DBD (8 min). These results demonstrate that fusion of the Pip and PU.1 DBDs created a protein which bound DNA with much greater stability than wild-type PU.1 or its DBD. In addition, the significantly longer half-life of the Pipmut–DNA complex (60 min) as compared with that of the PUmut–DNA complex (6 min) suggests that PipPU's binding stability depended on Arg232 and Arg235 of the PU.1 DBD. Similar experiments revealed that the half-life of the PU.1–Pip ternary complex was nearly identical to that of PU.1 alone (data not shown), suggesting that the elevated DNA-binding affinity of the ternary complex, as compared with PU.1, is due to an increased rate of association.

Wild-type, Pipmut and PUmut chimeras repress λ enhancer function in transient assays

For initial functional analyses, we transiently transfected expression plasmids containing PipPU, Pipmut, PUmut or the DM chimeras into the MPC-11 B cell line along with CAT reporter constructs driven by the $V_{\lambda 1}$ promoter with or without the λ enhancer, $E_{\lambda 2\text{-}4}$ (Figure 7A). Previous work has shown that the $E_{\lambda 2\text{-}4}$ construct (OPC 20) is preferentially active in B cells, and mutations in either the PU.1- or Pip-binding site within this construct abolish enhancer function (Eisenbeis *et al*., 1993). Consistent with previous data, the presence of $E_{\lambda 2\text{-}4}$ stimulated transcription 12-fold. Enhancer activity was strongly inhibited by expression of the PipPU, Pipmut and PUmut, but not by the DM fused dimer (Figure 7A). Comparable levels of all four

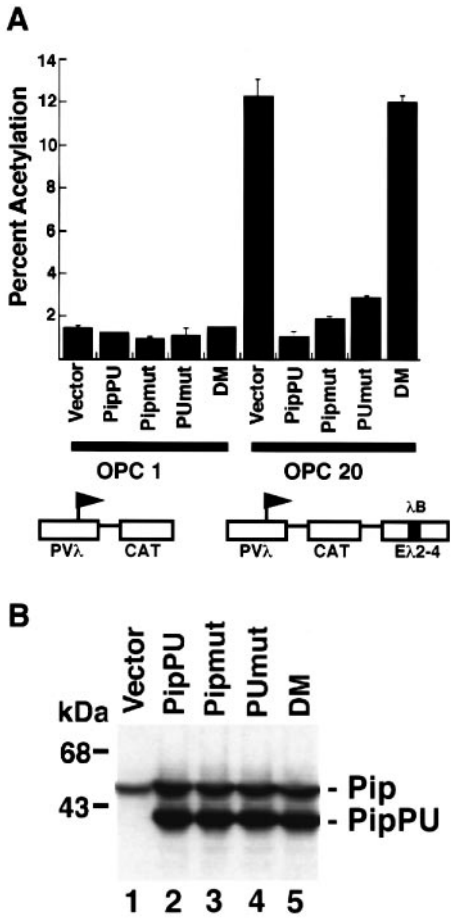

Fig. 7. Both wild-type and mutant PipPU chimeras repress λ enhancer function in transient transfection assays. (**A**) MPC-11 B cells were transiently transfected with the indicated expression constructs and either the OPC-1 or OPC-20 reporters. Solid bars indicate average CAT activity (percentage chloramphenicol acetylation) of two independent transfections. Error bars denote standard deviation. The structures of the indicated reporter constructs are shown below. (**B**) Western blot analysis of MPC-11 B cells transiently transfected with the indicated expression constructs. The blot was probed with anti-Pip antiserum. The positions of endogenous Pip protein and the transiently expressed PipPU chimeras are indicated.

chimeric proteins were expressed in transfected cells as determined by Western blotting (Figure 7B). The PipPU protein was somewhat more effective at blocking reporter gene activity as compared with the PUmut or Pipmut proteins. Furthermore, transcriptional repression by PipPU was specific, since it did not inhibit the activity of a reporter construct containing a Vκ promoter and the intron κ enhancer ($E_{i\kappa}$; data not shown). Therefore, in transient assays, both the wild-type (PipPU) and mutant chimeras (Pipmut and PUmut) effectively blocked enhancer function, presumably by displacement of endogenous PU.1–Pip complexes.

The PipPU chimeric repressor blocks endogenous IgL λ gene expression when stably expressed in B cells

The transient assays suggested that both PipPU and the mutant chimeras (PUmut and Pipmut) might inhibit the transcription of an endogenously rearranged IgL λ gene. To test this, we generated J558L B cells which stably express either the PipPU, Pipmut or PUmut proteins, using retroviral transduction. We chose the J558L plasma cell line because it expresses a functionally rearranged Vλ1–Jλ1 IgL allele (Figure 8C; Oi *et al*., 1983). Gel supershift assays have shown that PU.1 and Pip represent the major components of the ternary complex formed with nuclear extract from these cells (Brass *et al*., 1996). J558L B cells also express the J chain gene, the transcription of which has been suggested to be regulated by PU.1 binding to the J chain promoter (Shin and Koshland, 1993). Analysis of the effect of the wild-type repressor on the expression of the IgL λ and J chain genes would test whether their activity is indeed regulated by PU.1 *in vivo*. Parallel analyses with the mutant repressors would enable this approach to distinguish genes regulated by PU.1 and Pip (IgL λ) from those regulated by PU.1 alone (J chain).

Individual J558L clones that expressed similar levels of the chimeric proteins were identified by Western blotting using anti-Pip antiserum (Figure 8B, top). Each of the chimeric proteins was expressed comparably with endogenous Pip and their expression did not alter wild-type Pip levels (Figure 8B, top). Since the chimeras and wild-type PU.1 migrate similarly in denaturing gels, we used an anti-PU.1 antiserum which does not recognize the chimera to determine that expression of the fusion proteins had not altered endogenous PU.1 levels (Figure 8B, middle). An additional antiserum directed against the PU.1 ets domain showed that the chimeric proteins were expressed at considerably higher levels than endogenous PU.1 (Figure 8B, bottom). Gel shift assays using nuclear extracts from the stably transduced cell lines showed that the PipPU and mutant chimeras formed complexes with λB DNA to similar levels (data not shown).

Northern analysis of total RNA from two clones of each type was performed to assess levels of IgL λ and J chain gene transcripts (Figure 8A). β-actin transcripts were used both as a specificity control and for normalization. Strikingly, the wild-type chimera (PipPU) potently repressed endogenous IgL λ gene expression (17-fold). This repression was dependent on both the PU.1 and Pip DBDs, since the Pipmut or PUmut mutant chimeras inhibited less effectively (5.5- and 1.8-fold repression, respectively). These results establish that PU.1–Pip complexes are essential for the expression of a productively rearranged immunoglobulin λ gene in a plasma cell.

Transcription of the J chain gene was inhibited 3.5-fold by the wild-type PipPU chimera. Unlike the case with the IgL λ gene, the J chain gene was repressed equivalently by the wild-type and Pipmut repressors. It is important to note that J chain gene transcription was not inhibited by the PUmut chimera. Therefore, these data demonstrate that PU.1 alone is required for J chain gene activity. Furthermore, the overall analysis establishes the utility of using the PipPU fused dimer and its variants to distinguish genes regulated by PU.1 and Pip from those regulated by PU.1 alone.

Discussion

Cooperative binding by PU.1 and Pip is regulated by multiple interdependent DNA–protein and protein–protein interactions

Our experiments have focused on understanding the structural determinants underlying PU.1–Pip ternary complex

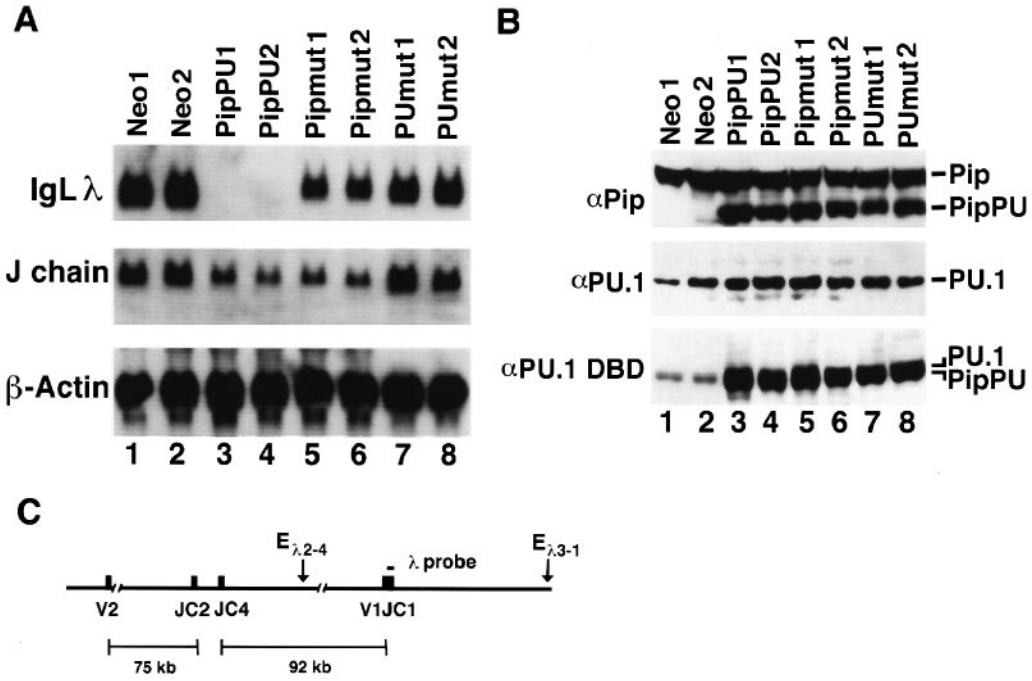

Fig. 8. The wild-type PipPU chimera potently inhibits endogenous immunoglobulin λ gene expression when stably expressed. (**A**) J558L B cells were transduced with retroviral vectors encoding the wild-type PipPU or mutant chimeras. Neo clones denote cells transduced with the parent vector. Individual clones (numbered as 1 and 2) were selected on the basis of equivalent levels of expression of the PipPU proteins. These clones were analyzed by Northern blotting for expression of IgL λ (top), J chain (middle) or β-actin (bottom) transcripts. These data are representative of three independent experiments each using different RNA preparations. (**B**) Western blot analysis of J558L B cell clones stably expressing the indicated PipPU proteins using anti-Pip (top), anti-PU.1 (middle) or anti-PU.1 DBD (bottom) antisera. In the bottom panel, endogenous PU.1 and the PipPU chimeras are seen to migrate as a tight doublet. (**C**) Schematic diagram of the functionally rearranged IgL λ locus (Vλ1–Cλ1) expressed by the J558L B cells. All DNA segments are drawn approximately to scale, with the physical distances indicated below and with solid boxes denoting exons (Hagman *et al*., 1990). The positions of $E_{\lambda 2\text{-}4}$ and $E_{\lambda 3\text{-}1}$, as well as the region recognized by the λC1 probe used in this study, are indicated.

formation. Previously, we identified a predicted α-helix within Pip's C-terminus (amino acids 395–413) that is critical for both formation of a ternary complex and autoinhibition of DNA binding (Brass *et al*., 1996). This helix is also required for transcriptional co-activation. A Pip deletion mutant, Pip 1–410, which does not form a ternary complex with PU.1 fails to activate transcription synergistically with PU.1. The alanine substitution study demonstrated that Arg398, Lys399 and Leu400, located within this predicted helix and conserved between Pip and ICSBP, are critical for PU.1–Pip interaction *in vitro* and *in vivo* (Figure 9B). Substitution of Lys399 by arginine partially restored complex formation, showing that a positively charged residue at this site is an important structural component of the complex. Both ICSBP and p48 contain similar residues in respective regions shown by deletional analyses to be vital for either interaction of ICSBP with IRF-2 (Sharf *et al*., 1997) or p48's association with STAT1 and STAT2 (Veals *et al*., 1993; Figure 9B). Therefore, such residues may play a more general role in IRF-containing complexes, including those involving IRF-3 (Au *et al*., 1995; Wathelet *et al*., 1998).

An interaction analogous to the one between PU.1 and Pip, involving the pKID domain of the CREB transcription factor and the KIX domain of the co-activator CBP, is mediated by a phosphoserine residue located within pKID (Parker *et al*., 1996). The solution structure of these heterodimerized domains indicates that a single hydrogen bond between this phosphoserine and a tyrosine residue within CBP is critical for complexation (Radhakrishnan *et al*., 1997). Moreover, three α-helices in the KIX domain

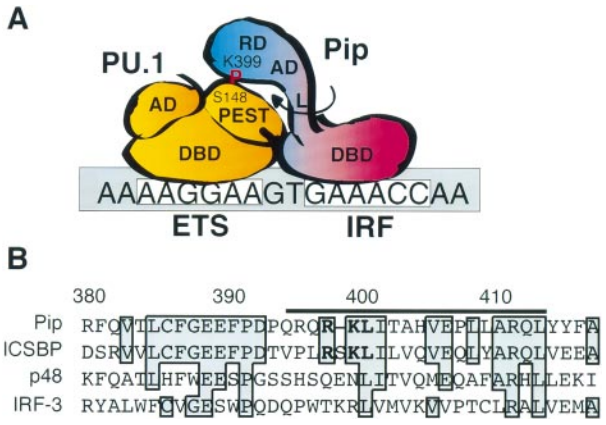

Fig. 9. Model of PU.1–Pip ternary complex formation. (**A**) Pip's regulatory domain (RD, amino acids 170–450) autoinhibits DNA binding by masking the Pip DBD. Interaction of Pip with a PU.1–DNA template complex causes the regulatory domain to swivel about the flexible linker region (L) and contact PU.1's PEST region. This contact is mediated by multiple residues in Pip's interaction helix, including an electrostatic interaction between K399 of Pip and PU.1's pSer148 (P-S148). Additional contacts between Pip's DBD and PU.1's DBD stabilize the ternary complex. (**B**) Protein sequence alignment of IRF interaction regions, with shaded boxes indicating residues conserved between Pip and ICSBP. Residues in p48 or IRF-3 that are also conserved with both Pip and ICSBP are also shaded. Pip's Arg398, Lys399 and Leu400 and the corresponding residues in ICSBP are in bold. The putative α-helix in Pip (amino acids 395–413) is overlined. Numbers along the top indicate locations in the protein sequence of Pip.

associate to form a pocket which accommodates the pKID domain by way of extensive hydrophobic contacts, interspersed with critical electrostatic interactions. In light of this study, our data suggest a possible mechanism for PU.1–Pip association involving an interaction between PU.1's pSer148 and Pip's Arg398 and Lys399. The ternary complex may also be stabilized by hydrophobic and/or polar contacts between Pip's Leu400, Ile401, Thr402 and His403, and PU.1. Finally, because a mutant Pip protein with an internal deletion of amino acids 150–340 cannot interact with PU.1 (Brass *et al*., 1996), it appears that other, as yet uncharacterized helices within this region may pack together with Pip's helix amino acids 395–413 to form a tertiary fold which is competent for PU.1 association.

Two biochemical properties of Pip's interaction helix, autoinhibition and PU.1 association, have been partially uncoupled in these studies. The mutant protein, PipAS397, is defective in its interaction with PU.1, but is autoinhibited. It is unlikely that the binding properties of PipAS397 are the result of misfolding of this polypeptide, because our proteolytic analysis shows that Pip is composed of two independent structural domains, a DBD domain and a regulatory domain, separated by a flexible linker. Thus, a mutation in Pip's regulatory domain should not perturb the structure of its DBD. Mutations in a predominantly hydrophobic patch at the C-terminus of the helix (amino acids 401–408) resulted in alleviation of autoinhibition. We propose that this region inhibits binding by masking the DBD; however, further work will be required to dissect the actual mechanism of autoinhibition. Intriguingly, a biological role for autoinhibition of Pip's DNA binding is suggested by studies involving the stable transfection of full-length ICSBP or a truncated protein consisting of the DBD of ICSBP (Thornton *et al*., 1996). The ICSBP DBD strongly repressed both interferon (IFN)-stimulated gene expression and the anti-proliferative effects of IFN, while the full-length protein had little effect on these activities. In view of this, we propose that the biological function of autoinhibition is to prevent Pip and ICSBP from binding inappropriately to IFN-regulated promoters and enhancers. This autoinhibition is alleviated upon interaction with a specific partner, i.e. PU.1 or Spi-B, in the context of a composite regulatory element. Such autoinhibition might also be alleviated by post-translational modification. In this regard, we note that IRF-3 possesses a C-terminal autoinhibitory region. Regulated phosphorylation of this region upon viral infection stimulates DNA binding (Lin *et al*., 1998; Yoneyama *et al*., 1998).

The cooperative binding of Pip and PU.1 is largely dependent on the interaction between the phosphorylated PEST region of PU.1 and the regulatory domain of Pip; elimination of the regulatory domain results in an 800-fold drop in the affinity of Pip for the PU.1–DNA complex. Furthermore, glutaraldehyde cross-linking demonstrated that the protein–protein interaction is template directed, because PU.1–Pip cross-linked adducts are detectable only in the presence of cognate DNA. Interdependent protein–protein and protein–DNA contacts mediating ternary complex assembly are not unprecedented. In the NFAT–AP-1–DNA complex, the Rel homology region of NFAT and the bZip domain of AP-1 make extensive contacts with one another that are both necessary and sufficient for complex formation on DNA (Chen *et al*., 1998). However, cross-linking experiments have shown that NFAT–AP-1 adducts are detectable only in the presence of specific DNA, arguing that protein–protein interactions alone are of insufficient strength for productive complexation (Chen *et al*., 1995). In both of these instances, transcription-activating complexes form only upon interaction of the appropriate partners and cognate DNA, thus ensuring the specific regulation of a distinct set of genes. A recent study using protein–protein interaction assays suggests that PU.1 and Pip can interact in the absence of template DNA (Perkel *et al*., 1998). The inability of our cross-linking assays to detect such an interaction is consistent with template DNA stabilizing weak protein–protein contacts between PU.1 and Pip.

We also detected an additional, albeit much weaker, cooperative interaction between Pip's DBD and PU.1's DBD. Subsequent assays suggested that this interaction was specific, because a Pip homolog, IRF-1, bound competitively with PU.1 on the λB site. As noted, in the PU.1 DBD–DNA co-crystal structure, the N-terminus of PU.1 is adjacent to the predicted binding site of Pip. It follows then that in the wild-type ternary complex, both the N-terminus of PU.1's DBD (amino acids 160–272) and its PEST region (amino acids 119–159) would be in position to contact Pip. When analyzed in the context of the wild-type PU.1–Pip complex, it is likely that the interaction between the DBDs will be found to be an important component of ternary complex formation.

Together, these experiments have allowed us to test and thereby extend our earlier model of PU.1–Pip interactions (Figure 9A; Brass *et al*., 1996). (i) Pip's regulatory domain autoinhibits DNA binding by masking the DBD via direct hydrophobic contacts. (ii) Upon interaction of Pip with PU.1 and DNA, Pip undergoes a conformational change involving the swiveling of its regulatory domain (amino acids 170–450) away from its own DBD, and into direct contact with PU.1's PEST region. This association is dependent on multiple residues within Pip's interaction helix, including an electrostatic interaction between Pip's Lys399 and PU.1's pSer148. (iii) Protein–protein contacts also occur between Pip's DBD and PU.1's DBD and may contribute additional specificity and stability to the ternary complex. Thus, we propose that PU.1–Pip ternary complex assembly is regulated by two template-directed protein–protein contacts, one between PU.1's PEST region and Pip's regulatory domain, and the second depending on association of PU.1's DBD with that of Pip. Once assembled on an enhancer or promoter *in vivo*, the PU.1–Pip complex may be stabilized by additional specific contacts with neighboring factors bound to adjacent sites. Based on the biochemical similarities between Ets–IRF complexes containing either PU.1 or Spi-B and Pip or ICSBP, we believe this model provides general insight into the concerted action of these transcription factors in both lymphoid and myeloid lineages.

Two IRF subgroups that are structurally and biochemically distinguishable

Our experiments involving the Pip and IRF-1 DBDs highlighted a crucial difference in the DNA-binding properties of IRF family members: the prototypical members of the IRF family, IRF-1 and IRF-2, bind to DNA with high affinity. However, Pip, ICSBP and p48 possess considerably lower DNA affinity, relying on partners to form high affinity

complexes. The recent IRF-1–DNA co-crystal structure (Escalante *et al*., 1998) reveals that in addition to the specific base contacts made by the recognition helix, IRF-1 makes extensive contacts with DNA backbone phosphates, even as far as six nucleotides upstream of the GAAA recognition core. Comparison of the IRF recognition site (GAGAAGT**GAAA**GT, IRF-1 core in bold) with the λB EICE (A**AGGA**GTGAAACC, PU.1 core emboldened) indicates that IRF-1's DNA backbone phosphate contacts straddle the PU.1-binding site, suggesting that the binding interference between PU.1 and IRF-1 results from the two proteins competing for binding to overlapping sites. In addition, the formation of IRF-1 dimers (Figure 4) raises the possibility that binding of a second IRF-1 molecule may directly force PU.1 off the DNA. If these IRF-1–DNA contacts allow high affinity binding and exclusion of PU.1, then partial loss of these interactions may account for the attenuated binding of Pip, ICSBP and p48. Moreover, a binding partner, such as PU.1 or STATs, may provide these lost contacts to Pip or p48 *in trans*, via protein–protein interactions. Future work should clarify how attenuation of DNA binding of a prototypic IRF domain resulted in the evolution of a distinct subgroup of factors, including Pip and ICSBP. The dependence of this subgroup on a DNA-binding partner creates additional specificity in gene regulation, thereby expanding the utility of the IRF DBD.

Engineering PU.1–Pip chimeric repressors

Previous studies have either created chimeric transcription factors which recognize synthetic regulatory elements by fusing domains from biologically unrelated proteins, or used phage display technology to create a zinc finger protein which recognizes a DNA site generated by a chromosomal translocation (Choo *et al*., 1994; Pomerantz *et al*., 1995). We have used a variation of the former approach to analyze the biological activity of an endogenous complex, PU.1–Pip. Our goal was to create a chimera from the isolated DBDs of these interacting proteins, PipPU, that preferentially recognized composite DNA elements, thereby allowing us to analyze the role of PU.1–Pip complexes in gene expression.

We constructed the chimera by fusing the PU.1 and Pip DBDs using a tandem repeat of the POU domain linker from the Oct-2 protein. The POU domain linker may be of general use for constructing chimeras, especially when lack of structural data precludes the calculation of optimal linker length. In addition, proteins containing this linker were found to be stable in both transient and stable expression systems, suggesting that this linker may be generally resistant to proteolysis *in vivo*. Our strategy produced a chimera, PipPU, which preferred a composite site to a PU.1 site by a factor of 3 (λB) or 8 (CD20), correlating with the affinity of wild-type PU.1 for these sites. This is consistent with the overall selectivity of a chimeric transcription factor depending on the intermediate affinity and high specificity of the isolated sub-domains (Pomerantz *et al*., 1995). The PipPU chimera bound the λB site less well than the wild-type proteins; however, on a composite element containing a lower affinity PU.1 site, the chimera and PU.1–Pip bound equivalently. These results suggest that additional conformational changes necessary for cooperativity may occur in the context of the native complex that are not recapitulated within PipPU. On lower affinity sites, however, the chelating effect provided by the linker may lower the overall entropic cost associated with binding, allowing PipPU to bind as efficiently as the wild-type proteins (Klemm and Pabo, 1996). Furthermore, kinetic analysis demonstrated that fusion of the two DBDs greatly enhanced DNA-binding stability as compared with wild-type PU.1 or PU.1–Pip, most likely due to the increased protein–DNA contacts elevating the free energy of interaction. Mutation of two residues important for sequence-specific recognition by the Pip DBD resulted in the Pipmut protein, which bound DNA with similar specificity to PU.1, but with a longer half-life. On the other hand, the PUmut protein, which contains mutations within the PU.1 DBD, independently bound DNA with high affinity and thus acted quite differently from Pip. The independent binding of PUmut may arise from phosphate backbone contacts provided by PU.1's DBD, which stabilize the weak DNA-binding activity of the Pip DBD. This last suggestion is supported by the numerous protein–DNA backbone contacts observed in the PU.1–DNA co-crystal structure (Kodandapani *et al*., 1996). Although the affinity of PUmut for λB DNA was similar to that of PipPU and Pipmut, the stability of the respective protein–DNA complexes was quite distinct. (Figure 6C and D). The PUmut dimer formed a protein–DNA complex that was considerably less stable (half-life = 6 min) as compared with those complexes containing PipPU or Pipmut (half-life = 60 min). Thus the kinetic stability of the fused dimer–DNA complexes correlates with their ability to repress transcription *in vivo* (see below).

PipPU chimeras repress both λ enhancer function and expression of a rearranged IgL λ gene

Despite the differences in specificities and affinities detected by gel shift assays, all three PipPU chimeras (PipPU, Pipmut and PUmut) repressed transcription of a λ enhancer-containing reporter in transient assays, with PipPU being somewhat more effective than the mutant chimeras. However, upon testing the effects of these proteins on endogenous IgL λ gene transcription in stably expressing cells, significant differences in their function were found, with maximal repression depending on the presence of both wild-type Pip and PU.1 DBDs. Our gel shift studies revealed that both DBDs contribute to the higher combined affinity and selectivity of the PipPU chimera as compared with either of the mutants. Therefore, in the stably transduced cells, PipPU's enhanced DNA-binding properties may allow it to locate more effectively a small number of endogenous EICEs, including the ones contained in the IgL λ enhancers. Once PipPU locates an EICE-containing enhancer, the stable binding of both its DBDs may be necessary to compete with endogenous Ets and IRF proteins for site occupancy. In addition, recent work has shown that PU.1 nucleates a multi-transcription factor complex on the $E_{\kappa 3'}$ (Pongubala and Atchison, 1997). Like $E_{\kappa 3'}$, $E_{\lambda 2\text{-}4}$ and $E_{\lambda 3\text{-}1}$ also contain juxtaposed binding sites occupied by multiple factors (Rudin and Storb, 1992). It is conceivable, therefore, that the correct docking of both PU.1's and Pip's DBDs on DNA permits PipPU to contact one or several neighboring transcription factors, resulting in a higher order complex that is transcriptionally inactive due to the absence of the activation domains of PU.1 and Pip (Thanos and Maniatis, 1995; Tanaka, 1996). Thus, it is likely that the differential DNA-binding properties of the chimeric proteins account

for their varying abilities to repress endogenous IgL λ gene transcription. It should be noted that in transient assays, the Pipmut and PUmut chimeras repressed transcription similarly to the wild-type chimera. This may be attributable to the higher ratio of target DNA to non-specific DNA as well as increased levels of protein expression in a transient assay.

Our study establishes the functional requirement for PU.1–Pip complexes for expression of the IgL λ locus in a plasma cell. Transcription of a rearranged IgL λ gene appears to be regulated by two enhancers, $E_{\lambda 2\text{-}4}$ and $E_{\lambda 3\text{-}1}$, which share high sequence identity. Each enhancer contains an essential composite site (λB) bound by PU.1 and Pip (Hagman *et al*., 1990; Rudin and Storb 1992; Eisenbeis *et al*., 1993). The PipPU fused dimer probably represses IgL λ gene transcription by disrupting the function of both λ enhancers via the displacement of PU.1–Pip complexes. Pip-deficient animals develop normal numbers of B cells (including λ-expressors) which cannot undergo activation (Mittrucker *et al*., 1997). Thus, Pip is dispensable for IgL λ transcription during B cell development but may be required for the enhanced expression of this locus during B cell activation and terminal differentiation. This is consistent with increased expression of Pip in plasma cell lines such as J558L (Brass *et al*., 1996).

Fused dimers as a general tool for analysis of combinatorial control of transcription in vivo

When stably expressed, PipPU repressed an EICE-containing gene, IgL λ, more efficiently than the mutant chimeras, demonstrating that PU.1–Pip complexes are essential for IgL λ expression *in vivo*. Transcription of the J chain gene was also inhibited by the wild-type PipPU chimera. This is presumably due to displacement of endogenous PU.1 from an isolated Ets site in the J chain promoter (Shin and Koshland, 1993). However, the J chain gene was repressed equivalently by the wild-type and Pipmut repressors. Therefore, unlike the case with the IgL λ gene, PU.1 alone is required for J chain gene activity. It is important to note that the combined analysis of the wild-type dimer with a series of mutants allowed us to distinguish genes regulated by PU.1 and Pip from those regulated by PU.1 alone. Therefore, this approach not only serves to test the proposed functions of interacting activators *in vivo*, but should also enable the identification of novel genes specifically regulated by such activator complexes. In addition, a variation of our approach may be applicable to the analysis of transcription factors which bind adjacent sites, but do not physically interact. This would permit the functional analysis of diverse combinatorial interactions among transcription factors that regulate distinct patterns of gene expression.

Materials and methods

Plasmids

Histidine-tagged PU.1 (amino acids 119–272), PU.1S148A (119–272), PU.1 DBD (160–272), Pip (1–450), PipK399A (1–450) and Pip DBD (1–134) were prepared by PCR amplification of relevant cDNA segments with *Pfu* polymerase (Stratagene). PU.1 and PU.1S148A fragments were digested with *Bam*HI and *Eco*RI and subcloned into pBac-2cp (Novagen). PU.1 DBD, Pip, PipK399A and Pip DBD were digested with *Bam*HI and subcloned into pET-15b (Novagen). Pip 1–419 was constructed by *Pfu* PCR and subcloned into the *Not*I and *Xba*I sites in pcDNA3-HA (Brass *et al*., 1996). The PipPU chimera was prepared using PCR and consists of an N-terminal Pip (amino acids 1–150) *Not*I–*Bam*HI fragment connected to a *Bam*HI–*Xba*I fragment containing a tandem repeat of the Oct-2 POU domain linker (amino acids 265–291, Muller *et al*., 1988) and the PU.1 DBD (amino acids 160–272) cloned into pcDNA3-HA. Site-directed mutagenisis of pcDNA3-HAPip and the PipPU chimeras (Pipmut, PUmut and DM) was done as described (Brass *et al*., 1996). PipPU, Pipmut and PUmut were blunt-end ligated into the *Hpa*I site of the MSCV-neo retroviral vector (Hawley *et al*., 1994) The structures of all constructs were confirmed by dideoxy sequencing. Other constructs used in this study have been described previously: PU.1/CMV (Eisenbeis *et al*., 1995), and Pip 1–439, Pip 1–410 and Pip 1–380 (Brass *et al*., 1996).

Protein purification

Pip, PipK399A, Pip DBD and PU.1 DBD were transformed into BL21(DE3)pLysS (Novagen). The cultures were incubated at 37°C and induced with 1 mM isopropyl-β-D-thiogalactopyranoside (IPTG). Cells were resuspended in 5 ml of buffer A (20 mM phosphate, 0.4 M NaCl, pH 7.5) with 60 mM imidazole, 20 mM 2-mercaptoethanol. The resuspended cells were sonicated and the lysate was cleared by centrifugation and loaded on a HiTrap chelating column (Pharmacia) charged with nickel. Proteins were eluted with buffer A with 200 mM imidazole, 10% glycerol, 0.1% NP-40. The proteins were >80% pure as judged by densitometric analysis of Coomassie Blue-stained 12.5% SDS–PAGE gels. PU.1 and PU.1S148A baculoviruses were produced by standard calcium phosphate transfection of Sf-9 cells using BacVector-2000 triple cut viral DNA (Novagen). Infected Sf-9 cells were processed identically to *E.coli* cells for protein purification. Gel shift analyses of these purified proteins confirmed that they possesed similar specific activities to their mammalian counterparts. IVT proteins were prepared and quantitated as previously described (Brass *et al*., 1996).

Gel mobility shift assays

The DNA-binding reaction conditions were as previously described (Eisenbeis *et al*., 1993) with the following modifications; 4.0 μg of poly(dI–dC) per reaction (Figures 1 and 6) or 0.25 μg of poly(dI–dC) per reaction (Figures 2–5). DNA-binding reactions (Figures 1 and 2) contained $2\text{–}4\times10^{-14}$ mol of IVT protein and 2.5×10^{5} c.p.m. of probe ($\sim8\times10^{-14}$ mol). Binding reactions were electrophoresed in a 1× TGE 5% polyacrylamide gel at 200 V. Quantitation of gel shifts was performed using a PhosphorImager system (Molecular Dynamics). Each determination represents the average of at least three independent experiments. Dissociation constants were determined by mathematical modeling of gel mobility shift assay data using non-linear least-squares analysis and the following relationship, $K_d = ([P]_t - [D]_b)[D]_f/[D]_b$, where $[P]_t$ is total protein, $[D]_b$ is bound DNA and $[D]_f$ is free DNA. In the case of a ternary complex, $[D]_f$ is unbound DNA and the PU.1–DNA complex, and $[D]_b$ is the ternary complex only. For kinetic assays, binding reactions containing IVT proteins and radiolabeled λB probe were incubated for ~40 min at room temperature, at which point a 1000-fold excess of unlabeled λB probe was added. Aliquots were removed at 0, 1, 5, 10, 15, 20 and 30 min time points and loaded on a running gel. The dissociation rate constant, k_{-1}, was determined by least-squares analysis of the equation $\ln[\text{bound}_t]/[\text{bound}_0] = -k_{-1}t$, where bound_t is the protein–DNA complex at each time point, bound_0 is the protein–DNA complex present at time zero, and t is the time of aliqout removal after the addition of unlabeled probe.

Partial proteolysis of Pip

Purified Pip protein (25 nM) was incubated with 0.3 ng/μl of sequencing grade chymotrypsin (Boehringer Mannheim) in 10 mM Tris–HCl (pH 7.5), 50 mM NaCl, 1 mM dithiothreitol (DTT), 1 mM EDTA and 0.1% NP-40 for 20 min at 25°C in the absence or presence of 100 nM PU.1 and 50 nM annealed λB DNA. Chymotrypsin was inactivated with 2% SDS and 100 mM DTT, and the reaction products were incubated at 95°C for 5 min. Proteolytic fragments were resolved on a 12.5% SDS–PAGE gel for Western analysis. Edman degradation sequencing was done by the University of Chicago Protein-peptide core (Applied Biosystems).

Western blot analysis

Western blot analysis was performed as described (Brass *et al*., 1996) using the following reagents: anti-Pip DBD is a polyclonal affinity-purified rabbit antiserum which recognizes Pip amino acids 1–150 (Brass *et al*., 1996), anti-Pip CTD (Santa Cruz) is a polyclonal affinity-purified goat antiserum raised against Pip amino acids 433–449, anti-PU.1 is a polyclonal affinity-purified rabbit antiserum which recognizes PU.1 amino acids 1–160 (Brass *et al*., 1996), and anti-PU.1 DBD (Santa Cruz) is a polyclonal

affinity-purified rabbit antiserum raised against PU.1 amino acids 251–271. His-tagged Pip was detected using an Ni-NTA horseradish peroxidase (HRP) conjugate (Qiagen). HA-tagged constructs were assayed using the 12CA5 anti-HA monoclonal antibody (Boehringer Mannheim).

Glutaraldehyde cross-linking assays

Reactions contained 8 nM purified Pip or PipK399A, 4 nM purified PU.1 or PU.1S148A, 10 mM phosphate (pH 7.5), 100 mM NaCl, 5% glycerol and 0.1% NP-40, with or without the indicated annealed probe in a total volume of 100 μl. Reactions were incubated at room temperature for 20 min. Glutaraldehyde (Sigma) was then added to 0.005% (v/v) for 10 min. Standard SDS–PAGE loading buffer was added, and the reactions were incubated at 95°C for 5 min and resolved in a 10% SDS–PAGE gel for Western analysis.

Transient transfection analysis

NIH 3T3 fibroblasts and MPC-11 B cells were transfected by standard calcium phosphate-mediated precipitation using 20 μg of total DNA, 1–10 μg of the indicated expression vector, 2.5 μg of the B4-TKCAT, OPC-1 or OPC-20 reporters (Eisenbeis *et al*., 1993; Shah *et al*., 1997) and 1 μg of an RSV-luciferase reference plasmid, with the balance made up with the empty expression vector. After 48 h, cells were lysed and CAT assays were performed as described after normalization for luciferase activity, and quantitated by PhosphorImager (Brass *et al*., 1996).

Retroviral production and transduction of cell lines

ϕNX-Eco retroviral packaging cells (Kinsella and Nolan, 1996) were transfected using standard calcium phosphate-mediated precipitation with 25 μg of expression vector DNA. Retroviral supernatants were collected at 24 h and used to transduce J558L cells in the presence of 5 μg/ml polybrene for 3 h. Cells were then cultured for 48 h, at which point cell lines were derived using limiting dilution and selection with 2 mg/ml G418 (Gibco-BRL).

Northern blot analysis

Total RNA was isolated from 10^7 cells using RNAzol (Tel-Test). MOPS/formaldehyde gel electrophoresis was done using 20 μg of total RNA per sample. RNA was transferred to a Hybond membrane (Amersham) and probed using Rapid-hyb buffer (Amersham). cDNA probes for Cλ1, J chain and β-actin were generated using random prime labeling of purified fragments with [α-^{32}P]dCTP. The J chain probe consisted of a 1.2 kb *Xba*I fragment from a 3.9 kb J chain cDNA (pcJX). The Cλ1 probe consisted of a 158 bp *Bst*N1 fragment subcloned from pClambda 1 (Miller *et al*., 1981).

Acknowledgements

We are extremely grateful to Will Chutkow, Dan Oppenheimer, Paula Loria and Doug Hattendorf for technical advice and reagents. We thank Laura Wilhelmi, Deborah Brass, Steven Kosak, Jon Walsh, Eric Bertolino, Erica Smith and Mike Palopoli for their critical review of the manuscript, and Gail Hubbard for help in manuscript preparation. We also thank Cheryl Arrowsmith (Ontario Cancer Institute, University of Toronto, Canada) for helpful discussion and communicating results prior to publication. In addition, we are indebted to Pratik Shah for valuable advice concerning the design of the chimeric repressor, and Aneel Aggarwal and Carlos Escalante (Mount Sinai Medical Center, New York, NY) for discussions of IRF structure and providing IRF-1 DBD protein. This work was supported by the Howard Hughes Medical Institute (A.Q.Z., A.L.B. and H.S.) and NIH training grant HD07009 (A.L.B.).

References

Au,W.C., Moore,P.A., Lowther,W., Juang,Y.T. and Pitha,P.M. (1995) Identification of a member of the interferon regulatory factor family that binds to the interferon-stimulated response element and activates expression of interferon-induced genes. *Proc. Natl Acad. Sci. USA*, **92**, 11657–11661.

Bender,A. and Sprague,G.F.,Jr (1987) MAT alpha 1 protein, a yeast transcription activator, binds synergistically with a second protein to a set of cell-type-specific genes. *Cell*, **50**, 681–691.

Brass,A.L. (1998) PU.1/Pip ternary complex formation. PhD thesis, University of Chicago, Chicago, IL.

Brass,A.L., Kehrli,E., Eisenbeis,C.F., Storb,U. and Singh,H. (1996) Pip, a lymphoid-restricted IRF, contains a regulatory domain that is important for autoinhibition and ternary complex formation with the Ets factor PU.1. *Genes Dev.*, **10**, 2335–2347.

Carey,M. (1998) The enhanceosome and transcriptional synergy. *Cell*, **92**, 5–8.

Chen,L., Oakley,M.G., Glover,J.N., Jain,J., Dervan,P.B., Hogan,P.G., Rao,A. and Verdine,G.L. (1995) Only one of the two DNA-bound orientations of AP-1 found in solution cooperates with NFATp. *Curr. Biol.*, **5**, 882–889.

Chen,L., Glover,J.N., Hogan,P.G., Rao,A. and Harrison,S.C. (1998) Structure of the DNA-binding domains from NFAT, Fos and Jun bound specifically to DNA. *Nature*, **392**, 42–48.

Choo,Y., Sanchez-Garcia,I. and Klug,A. (1994) *In vivo* repression by a site-specific DNA-binding protein designed against an oncogenic sequence. *Nature*, **372**, 642–645.

Chou,P.Y. and Fasman,G.D. (1978) Empirical predictions of protein conformation. *Annu. Rev. Biochem.*, **47**, 251–276.

Dalton,S. and Treisman,R. (1992) Characterization of SAP-1, a protein recruited by serum response factor to the c-*fos* serum response element. *Cell*, **68**, 597–612.

Driggers,P.H., Ennist,D.L., Gleason,S.L., Mak,W.H., Marks,M.S., Levi,B.Z., Flanagan,J.R., Appella,E. and Ozato,K. (1990) An interferon gamma-regulated protein that binds the interferon-inducible enhancer element of major histocompatibility complex class I genes. *Proc. Natl Acad. Sci. USA*, **87**, 3743–3747.

Eisenbeis,C.F., Singh,H. and Storb,U. (1993) PU.1 is a component of a multiprotein complex which binds an essential site in the murine immunoglobulin lambda 2–4 enhancer. *Mol. Cell. Biol.*, **13**, 6452–6461.

Eisenbeis,C.F., Singh,H. and Storb,U. (1995) Pip, a novel IRF family member, is a lymphoid-specific, PU.1-dependent transcriptional activator. *Genes Dev.*, **9**, 1377–1387.

Escalante,C.R., Yie,J., Thanos,D. and Aggarwal,A.K. (1998) Structure of IRF-1 with bound DNA reveals determinants of interferon regulation. *Nature*, **391**, 103–106.

Giese,K., Kingsley,C., Kirshner,J.R. and Grosschedl,R. (1995) Assembly and function of a TCRα enhancer complex is dependent on LEF-1-induced DNA bending and multiple protein–protein interactions. *Genes Dev.*, **9**, 995–1008.

Hagman,J., Rudin,C.M., Haasch,D., Chaplin,D. and Storb,U. (1990) A novel enhancer in the immunoglobulin lambda locus is duplicated and functionally independent of NF kappa B. *Genes Dev.*, **4**, 978–992.

Hawley,R.G., Lieu,F.H., Fong,A.Z. and Hawley,T.S. (1994) Versatile retroviral vectors for potential use in gene therapy. *Gene Ther.*, **1**, 136–138.

Herr,W. and Cleary,M.A. (1995) The POU domain: versatility in transcriptional regulation by a flexible two-in-one DNA-binding domain. *Genes Dev.*, **9**, 1679–1693.

Himmelmann,A., Riva,A., Wilson,G.L., Lucas,B.P., Thevenin,C. and Kehrl,J.H. (1997) PU.1/Pip and basic helix loop helix zipper transcription factors interact with binding sites in the CD20 promoter to help confer lineage- and stage-specific expression of CD20 in B lymphocytes. *Blood*, **90**, 3984–3995.

Holtschke,T. *et al*. (1996) Immunodeficiency and chronic myelogenous leukemia-like syndrome in mice with a targeted mutation of the ICSBP gene. *Cell*, **87**, 307–317.

Iida,S., Rao,P.H., Butler,M., Corradini,P., Boccadoro,M., Klein,B., Chaganti,R.S. and Dalla-Favera,R. (1997) Deregulation of MUM1/IRF4 by chromosomal translocation in multiple myeloma. *Nature Genet.*, **17**, 226–230.

Jain,J., McCaffrey,P.G., Valge-Archer,V.E. and Rao,A. (1992) Nuclear factor of activated T cells contains Fos and Jun. *Nature*, **356**, 801–804.

Kinsella,T.M. and Nolan,G.P. (1996) Episomal vectors rapidly and stably produce high-titer recombinant retrovirus. *Hum. Gene Ther.*, **7**, 1405–1413.

Klemm,J.D. and Pabo,C.O. (1996) Oct-1 POU domain–DNA interactions: cooperative binding of isolated subdomains and effects of covalent linkage. *Genes Dev.*, **10**, 27–36.

Klemm,J.D., Rould,M.A., Aurora,R., Herr,W. and Pabo,C.O. (1994) Crystal structure of the Oct-1 POU domain bound to an octamer site: DNA recognition with tethered DNA-binding modules. *Cell*, **77**, 21–32.

Kodandapani,R., Pio,F., Ni,C.Z., Piccialli,G., Klemsz,M., McKercher,S., Maki,R.A. and Ely,K.R. (1996) A new pattern for helix–turn–helix recognition revealed by the PU.1 ETS-domain–DNA complex. *Nature*, **380**, 456–460.

Lin,R., Heylbroeck,C., Pitha,P.M. and Hiscott,J. (1998) Virus-dependent phosphorylation of the IRF-3 transcription factor regulates nuclear translocation, transactivation potential and proteasome-mediated degradation. *Mol. Cell. Biol.*, **18**, 2986–2996.

Miller,J., Bothwell,A. and Storb,U. (1981) Physical linkage of the constant region genes for immunoglobulins lambda I and lambda III. *Proc. Natl Acad. Sci. USA*, **78**, 3829–3833.

Mittrucker,H.W. *et al*. (1997) Requirement for the transcription factor LSIRF/IRF4 for mature B and T lymphocyte function. *Science*, **275**, 540–543.

Muller,M.M., Ruppert,S., Schaffner,W. and Matthias,P. (1988) A cloned octamer transcription factor stimulates transcription from lymphoid-specific promoters in non-B cells. *Nature*, **336**, 544–551.

Nelson,N., Marks,M.S., Driggers,P.H. and Ozato,K. (1993) Interferon consensus sequence-binding protein, a member of the interferon regulatory factor family, suppresses interferon-induced gene transcription. *Mol. Cell. Biol.*, **13**, 588–599.

Oi,V.T., Morrison,S.L., Herzenberg,L.A. and Berg,P. (1983) Immunoglobulin gene expression in transformed lymphoid cells. *Proc. Natl Acad. Sci. USA*, **80**, 825–829.

Parker,D., Ferreri,K., Nakajima,T., LaMorte,V.J., Evans,R., Koerber,S.C., Hoeger,C. and Montminy,M.R. (1996) Phosphorylation of CREB at Ser-133 induces complex formation with CREB-binding protein via a direct mechanism. *Mol. Cell. Biol.*, **16**, 694–703.

Perkel,J.M. and Atchison,M.L. (1998) A two-step mechanism for recruitment of Pip by PU.1. *J. Immunol.*, **160**, 241–252.

Pomerantz,J.L., Sharp,P.A. and Pabo,C.O. (1995) Structure-based design of transcription factors. *Science*, **267**, 93–96.

Pongubala,J.M. and Atchison,M.L. (1997) PU.1 can participate in an active enhancer complex without its transcriptional activation domain. *Proc. Natl Acad. Sci. USA*, **94**, 127–132.

Pongubala,J.M., Nagulapalli,S., Klemsz,M.J., McKercher,S.R., Maki,R.A. and Atchison,M.L. (1992) PU.1 recruits a second nuclear factor to a site important for immunoglobulin kappa 3′ enhancer activity. *Mol. Cell. Biol.*, **12**, 368–378.

Pongubala,J.M., Van Beveren,C., Nagulapalli,S., Klemsz,M.J., McKercher,S.R., Maki,R.A. and Atchison,M.L. (1993) Effect of PU.1 phosphorylation on interaction with NF-EM5 and transcriptional activation. *Science*, **259**, 1622–1625.

Radhakrishnan,I., Perez-Alvarado,G.C., Parker,D., Dyson,H.J., Montminy, M.R. and Wright,P.E. (1997) Solution structure of the KIX domain of CBP bound to the transactivation domain of CREB: a model for activator:coactivator interactions. *Cell*, **91**, 741–752.

Ray,D., Bosselut,R., Ghysdael,J., Mattei,M.G., Tavitian,A. and Moreau-Gachelin,F. (1992) Characterization of Spi-B, a transcription factor related to the putative oncoprotein Spi-1/PU.1. *Mol. Cell. Biol.*, **12**, 4297–4304.

Rudin,C.M. and Storb,U. (1992) Two conserved essential motifs of the murine immunoglobulin lambda enhancers bind B-cell-specific factors. *Mol. Cell. Biol.* **12**, 309–320.

Scott,E., Simon,M., Anastasi,J. and Singh,H. (1994) Requirement of transcription factor PU.1 in the development of multiple hematopoietic lineages. *Science*, **265**, 1573–1577.

Shah,P.C., Bertolino,E. and Singh,H. (1997) Using altered specificity Oct-1 and Oct-2 mutants to analyze the regulation of immunoglobulin gene transcription. *EMBO J.*, **16**, 7105–7117.

Sharf,R., Azriel,A., Lejbkowicz,F., Winograd,S.S., Ehrlich,R. and Levi,B.Z. (1995) Functional domain analysis of interferon consensus sequence binding protein (ICSBP) and its association with interferon regulatory factors. *J. Biol. Chem.*, **270**, 13063–13069.

Sharf,R. *et al*. (1997) Phosphorylation events modulate the ability of interferon consensus sequence binding protein to interact with interferon regulatory factors and to bind DNA. *J. Biol. Chem.*, **272**, 9785–9792.

Shin,M.K. and Koshland,M.E. (1993) Ets-related protein PU.1 regulates expression of the immunoglobulin J-chain gene through a novel Ets-binding element. *Genes Dev.*, **7**, 2006–2015.

Su,G.H., Ip,H.S., Cobb,B.S., Lu,M.M., Chen,H.M. and Simon,M.C. (1996) The Ets protein Spi-B is expressed exclusively in B cells and T cells during development. *J. Exp. Med.*, **184**, 203–214.

Su,G.H., Chen,H.M., Muthusamy,N., Garrett-Sinha,L.A., Baunoch,D., Tenen,D.G. and Simon,M.C. (1997) Defective B cell receptor-mediated responses in mice lacking the Ets protein, Spi-B. *EMBO J.*, **16**, 7118–7129.

Tan,S. and Richmond,T.J. (1998) Crystal structure of the yeast MATα2/MCM1/DNA ternary complex. *Nature*, **391**, 660–666.

Tanaka,M. (1996) Modulation of promoter occupancy by cooperative DNA binding and activation-domain function is a major determinant of transcriptional regulation by activators *in vivo*. *Proc. Natl Acad. Sci. USA*, **93**, 4311–4315.

Thanos,D. and Maniatis,T. (1995) Virus induction of human IFN beta gene expression requires the assembly of an enhanceosome. *Cell*, **83**, 1091–1100.

Thornton,A.M., Ogryzko,V.V., Dent,A., Sharf,R., Levi,B.Z., Kanno,Y., Staudt,L.M., Howard,B.H. and Ozato,K. (1996) A dominant negative mutant of an IFN regulatory factor family protein inhibits both type I and type II IFN-stimulated gene expression and antiproliferative activity of IFNs. *J. Immunol.*, **157**, 5145–5154.

Veals,S.A., Santa Maria,T. and Levy,D.E. (1993) Two domains of ISGF3 gamma that mediate protein–DNA and protein–protein interactions during transcription factor assembly contribute to DNA-binding specificity. *Mol. Cell. Biol.*, **13**, 196–206.

Wathelet,M.G., Lin,C.H., Parekh,B.S., Ronco,L.V., Howley,P.M. and Maniatis,T. (1998) Virus infection induces the assembly of coordinately activated transcription factors on the IFN-beta enhancer *in vivo*. *Mol. Cell*, **1**, 507–518.

Yamagata,T., Nishida,J., Tanaka,T., Sakai,R., Mitani,K., Yoshida,M., Taniguchi,T., Yazaki,Y. and Hirai,H. (1996) A novel interferon regulatory factor family transcription factor, ICSAT/Pip/LSIRF, that negatively regulates the activity of interferon-regulated genes. *Mol. Cell. Biol.*, **16**, 1283–1294.

Yoneyama,M., Suhara,W., Fukuhara,Y., Fukuda,M., Nishida,E. and Fujita,T. (1998) Direct triggering of the type I interferon system by virus infection: activation of a transcription factor complex containing IRF-3 and CBP/p300. *EMBO J.*, **17**, 1087–1095.

Received September 29, 1998; revised December 10, 1998; accepted December 14, 1998